Majorana Zero Modes in Topological Quantum Computing: Error-Resistant Codes Through Dynamical Symmetries

@tsotchke

December 11, 2022

Abstract

Quantum computation can be realised physically in terms of topological zero modes of Majorana fermions: particles with the unique characteristic of having equivalent particle and anti-particle representations which obey Pauli spin-statistics. Pseudo-physical modes of these particles have been observed at the boundaries of topological semiconductors. Anyons are 2-dimensional quasiparticles which can model these so-called Majorana Zero modes as 4-D spacetime braids of Ising spin chains. The topological qubits represented by these braids can be used to perform universal quantum computation. We will consider the possible implementation of topological quantum computation via Majorana zero modes with examples from QisKit.

Contents

1 Introduction

Quantum Computing is a novel venture into a domain of scientific development which is fraught by many new challenges. This new science presents formidable barriers stretching the very limits of both human comprehension and technicality to understand and, eventually, overcome. In the pursuit of this new paradigm of computing many approaches have been undertaken. The earliest forays into quantum computing have primarily involved photonics, or polarisation-based qubits which involve optical qubits which are given as superpositions of states of photons. In this case, the photonic qubits are not essentially "real" objects in the conventional sense of the word, in so much as they are inseparable from the quantum channel in which they are represented. Photonic quantum computing is still in active development today.

However, our subject of interest today involves a new form of matter which arises in the pursuit of topological quantum computation. This so-called *Topological Matter* has no analogue to anything from the world of classical mechanics, but rather it is a purely quantum mechanical substance[15]. As such, we must adopt a new vernacular in order to make any kind of meaningful statements about this kind of material. From here we will begin with a basic summary of some of the new concepts from physics that we must introduce to describe TM, namely the notion of geometric phases from which we will further develop to understand the notion of invariants.

1.1 Formalism and Concepts

One of the many results which we will import from topological band theory in condensed matter physics is the notion of the Berry Phase. It is something of a generalisation of *fibre bundle holonomy* and describes a wide range of both classical and quantum mechanical phenomena, including the important *Aharonov-Bohm effect*[3]. This phase is primary to calculating statistics of anyons in many-body systems obeying canonical correlation mechanics. Classically, this holonomy can be considered as the transport of a normal vector rotated by some angle θ_Γ along some surface along a closed path Γ which is a simple, closed loop circuiting the topology.

2 Group Holonomy and Berry Phase

In the simplest case of a Möbius strip, this angle generates exactly two discrete outcomes $\theta_\Gamma = \{0, \pi\}$ which correspond to either the same or reversed orientation of the normal vector, respectively, to the surface topology and more generally as $\theta_\Gamma = \pi n_\Gamma (\text{mod } 2\pi)$ where n_Γ is the winding number corresponding to the number of complete loops about the path. This construction ordinarily describes the *geometric holonomy* of a surface, and in this particular case it is also the *topological holomony*[15] because it exposes the non-trivial topological robustness of the path with respect to deformative deviations in the vector transport. For a given quantum mechanical system with Hamiltonian H which takes some set of state parameter values $\mathbf{k}$ in the state space $\mathcal{H}$ we can define a basis for the physical state vectors in terms of the eigenvalues of $E_n(\mathbf{k})$ as:

$$H(\mathbf{k}) |n; \mathbf{k}\rangle = E_n(\mathbf{k}) |n; \mathbf{k}\rangle , \tag{1}$$

which is related to a family of solutions via the arbitrary rotation of the phase factor $|n; \mathbf{k}\rangle' \to e^{i\zeta_n(\mathbf{k})} |n; \mathbf{k}\rangle$. These *gauge transformations* correspond to the sole degree of freedom for the wave function with path phase angle $\gamma_n(t) = \int_0^t \mathrm{d}\mathbf{k} \cdot \mathcal{A}^n(\mathbf{k})$ and dynamical phase in the solution of the time-dependent Schrödinger equation:

$$\begin{aligned} i\hbar \frac{d}{dt} |\psi_n(t)\rangle &= H(\mathbf{k}(t)) |\psi_n(t)\rangle \\ &\Rightarrow |\psi_n(t)\rangle = e^{i\gamma_n(t)} e^{-\frac{i}{\hbar}\int_0^t \mathrm{d}t' E_n(\mathbf{k}(t'))} |n; \mathbf{k}\rangle . \end{aligned} \tag{2}$$

This gauge dependent quantity $\mathcal{A}^n(\mathbf{k}) = i \langle n; \mathbf{k}| \frac{\partial}{\partial \mathbf{k}} |n; \mathbf{k}\rangle$ is the *Berry connection* and transforms according to the evolution of the field curvature tensor as $\mathcal{A}^n(\mathbf{k}) \to \mathcal{A}^n(\mathbf{k}) - \frac{\partial}{\partial \mathbf{k}} \zeta_n(\mathbf{k})$. If we parametrise this transformation in three dimensions we find the gauge invariant *Berry Curvature* as $\Omega^n_{\mu\nu}(\mathbf{k}) = \epsilon_{\mu\nu\lambda} \Omega^n_\lambda(\mathbf{k})$, where $\epsilon_{\mu\nu\lambda}$ is the Levi-Civita tensor.

2.1 Aharonov-Bohm Effect

The Aharonov-Bohm phase[16] can be seen as a generalisation of the formalism of the Berry phase[7]. Simply, the ABE can be considered as the *geometric phase* γ_n acquired by a particle travelling along a closed contour in the presence of an external field which depends on the total magnetic flux passing through. In the presence of an adiabatic change the wave function transforms by a phase angle $|\psi_n(t)\rangle \to e^{i\gamma_n(t)}|\psi_n(t)\rangle$, similarly to what we have seen in the above section.

For a particle contained in a box, $\psi_n(\mathbf{r},\mathbf{R}) = e^{-\frac{iq}{\hbar}\int_{\mathbf{r}}^{\mathbf{R}}\mathbf{A}(\mathbf{k})\,\mathrm{d}\mathbf{k}}\psi_n^0(\mathbf{r}-\mathbf{R})$ with coordinates $\mathbf{r}' = \mathbf{r}-\mathbf{R}$ which is the respective position of the particle relative to the box, transported along a closed loop $\mathbf{R}(t) \in \mathcal{C}$ we find the Berry connection to be proportional to the vector potential of the flux of the magnetic field $\mathbf{B}(\mathbf{R}) = \nabla \times \mathcal{A}(\mathbf{R})$. This potential is zero everywhere except for the region occupying the infinitesimally small interior of the thin flux tube[15]. The corresponding geometric phase of this impenetrable flux tube is given for the Berry Connection $\mathcal{A}^n(\mathbf{R}) \to \frac{q}{\hbar}\mathbf{A}(\mathbf{R})$ as:

$$\gamma_{\mathrm{AB}}(\mathcal{C}) = \frac{q}{\hbar}\oint_{\mathcal{C}}\mathbf{A}\cdot\mathrm{d}\mathbf{R}. \tag{3}$$

2.2 Geometric Phase as Fibre Bundle Holonomy

If we consider a *base manifold* $\mathcal{M}$ over an *total space* E with an open set of *fibres* F_x to constitute a *fibre bundle* (also denoted E) then we may define a bijective projective mapping $\pi : E \to M$ such that each fibre $F_x = \pi^{-1}(x)$ is associated with a given point $x \in \mathcal{M}$. For any open neighbourhood $U_x \in \mathcal{M}$ we may "cover" the entire base space with a union of the members of the set $\{U_\alpha\}$ of open subsets, provided there is a pair of local coordinates (U_α, ϕ_α) called a chart, defined by a set of continuous diffeomorphisms $\phi_\alpha : \pi^{-1}(U_\alpha) \to U_\alpha \times F$.

If we consider a closed curve $\mathcal{C}_{\mathcal{M}}(t)$ on the base manifold $\mathcal{M}$ then we can define the connection ω to be a local one-form by the connection $\mathcal{A}_\alpha = s_\alpha^*\omega$, such that s_α^* is the *pull-back* of $s_\alpha : U_\alpha \to P$, the *principal fibre bundle*. For the path ordering operator $\mathcal{P}$ over a projective Hilbert space, we find the element $g \in G$ of the *holonomy group* in terms of the local one-form connection[13]:

$$g = \mathcal{P}e^{i\oint_{\mathcal{C}}\mathcal{A}} = \mathcal{P}e^{i\gamma}, \tag{4}$$

where $\mathcal{P} = 1$ if Abelian[15]. For a fibre bundle:

$$\lambda_{\mathbf{R}}^n = \{|\psi\rangle \in \mathcal{H} : |\psi\rangle = e^{i\phi}|n;\mathbf{R}\rangle, \phi \in [0, 2\pi]\} \tag{5}$$

constructed over $\mathcal{M}$ by the parameter space $\mathbf{R}(t)$ we find that any two eigenvectors differ only by a $U(1)$ phase factor such that $|n;\mathbf{R},\beta\rangle = e^{i\zeta_{\beta\alpha}(\mathbf{R})}|n;\mathbf{R},\alpha\rangle$.

The Berry phase $e^{i\gamma_n}$ is synonymous with the holonomy of the local connection $\mathcal{A}^n$ over λ^n. This feature characterises λ^n as the principal fibre bundle over $\mathcal{M}$. From this, we may construct the state vector for the projective mapping $\pi(|\psi\rangle) = \rho$ by the principal fibre bundle:

$$\eta_\rho = \{|\psi\rangle : |\psi\rangle \langle\psi| = \rho, \langle\psi|\psi\rangle = 1\}, \tag{6}$$

over the projective Hilbert space $\mathcal{P}(\mathcal{H})$ if and only if $|\psi\rangle \in \rho$. Finally, we are able to define the *Aharonov-Anandan phase* in terms of this lifting property:

$$\mathcal{C}_{AA} : \left|\tilde{\psi}\left(0\right)\right\rangle \rightarrow \left|\tilde{\psi}\left(t\right)\right\rangle = e^{i\gamma(t)} \left|\tilde{\psi}\left(0\right)\right\rangle . \tag{7}$$

Thus, the curve $\mathcal{C}_{AA}$ is an open path in the total space of the principal fibre bundle η_ρ that projects onto $\mathcal{C}$ in the projective Hilbert space $\mathcal{P}(\mathcal{H})$ which has now become the base manifold, such that g is a member of the $U(1)$ structure group connecting the initial and final points of $\mathcal{A}$ over η_ρ.

3 Symmetrical Properties

Symmetry rests at the very heart of physics itself. It is perhaps somewhat unsurprising, but there is more to the idea of expressing physical laws than merely the aesthetic appeal of writing equations as a devotion to simplicity and beauty. Symmetries in the laws of physics are used to simplify complex and often seemingly impossible problems by reducing them to their independent parameters. In the standard model of physics, Landau-Fermi liquid theory describes the process by which low-energy excitations of *quasiparticles* in a self-interacting Fermi system map injectively into a free system of excited fermion states[15]. These quasiparticles inherit the properties of their interactions but preserve their spin and momentum in terms of the renormalisation of the effective mass with the effective bipartite particle interaction.

The power of this formulation is how it can be generalised to a variety of arbitrary systems of low-energy excitations. These *emergent particles* are effective field observables, such as phonons which are themselves non-interacting bosons with energy-independent velocity. Other such *emergent properties* of a system treated in terms of its macroscopic degrees of freedom are the local *order parameters* of high-symmetry disordered phases, so-called *paramagnetism*, and low-symmetry ordered phases, so-called *ferromagnetism.* A tendency for a system's phase to transition under the variation of some certain parameter is referred to as *spontaneous symmetry breaking*. Indeed, if two systems have different phases of matter then they must necessarily have different symmetries. However, spontaneous symmetry breaking alone is not sufficient to determine the total state of every possible system. For example, the topological properties associated with *Fractional Quantum Hall* liquids are necessary to determine whether phases of matter can be connected continuously. In seeming defiance of Landau symmetry breaking, these FQH liquids may have the same symmetry but different phase transitions. Therefore it is necessary to consider an alternative property defined in terms of topological invariants to distinguish their states. However, in order to understand this necessary condition we must first develop a greater understanding of the mechanism through which local deformations of space-time resolve in spontaneous state collapse.

3.1 Landau Symmetry Breaking

For now, let us consider only topologically trivial spaces. We describe the mechanism of Landau symmetry breaking in terms of the measures of the "degree of order" of a system. For example, in the simple case of liquid-gas phase transition this is represented by a first-order transition corresponding to the weak distinction between the two phases of matter according to the temperature-pressure plane at the critical point. These states can practically be considered indistinguishable since there is no real qualitative difference between them, hence they are effectively one sole state.

For a more complex system with distinguishable states the *order parameter* in the broken symmetry phase of a given quantum system, given by $\psi(\mathbf{r})$, is ether equal to zero in the case of a disordered phase and non-zero for an ordered phase. The equilibrium thermodynamic quantity with respect to the order parameter is the average of a small local operator which is uniform near the phase transition. It is completely determined by the free energy of the minimised functional such that:

$$F[\psi(\mathbf{r}), T] = F_0(T) + F_L[\psi(\mathbf{r}), T], \tag{8}$$

where $F_0(T)$ is a smooth function of temperature and the Landau functional, $F_L[\psi(\mathbf{r}), T]$, is an analytic function usually written as a polynomial expansion of the order parameter which is necessarily invariant under all symmetries[15]. Goldstone's theorem states that each spontaneously broken *continuous global* symmetry corresponds to a massless quasiparticle called a *Goldstone boson*.

However, this theorem does not describe how discrete local symmetries are broken. By contrast to the global symmetries which act identically on every point in space of a given Hamiltonian, local symmetries describe stricter constraints of invariance with respect to symmetry operations of disordered phases under local group transformations such as systems of charge-coupled spin-1/2 fermions undergoing spontaneous symmetry breaking during transition to a state of superconductivity.

3.2 Ising Ferromagnetism

At low temperatures a paramagnetic crystal may spontaneously break its full spin-rotation symmetries with respect to an axially reduced symmetry parallel to the magnetisation. Such a change in state induces a ferromagnetic phase transition in the physical structure of the crystal. For a ferromagnetic phase the discrete time-reversal and inversion symmetries are spontaneously broken[17].

Consider the Hamiltonian of an Ising ferromagnet with a short-ranged coupling J_{ij}:

$$H_I = -\frac{1}{2}\sum_{i,j} J_{ij} S_i S_j. \tag{9}$$

This quantity is characterised by $\mathbb{Z}_2$ symmetry and is invariant under time-reversal for which $S_i = \pm 1 \to -S_i$. The spins described by this Hamiltonian tend to spontaneously break into either up or down states with average spin value $\psi = \langle S_i \rangle$. We may construct an effective lattice field theory for this quadratic Ising Hamiltonian using functional integral representation by the Hubbard-Stratonovich transformation[5]:

$$Z = \mathrm{Tr} e^{-\beta H_I} = A \prod_i \int \mathrm{d}\psi_i e^{-\frac{1}{2}\sum_{i,j}\psi_i K_{ij}\psi_j + \sum_i \ln[2\cosh(\sum_j K_{ij}\psi_i\psi_j + \beta h_i)]}, \tag{10}$$

with average value $\langle \psi_i \rangle = \partial \ln Z / \partial \beta h_i = \langle S_i \rangle$. By the usage of a *saddle-point approximation* we may approximate the free energy $F[T]$ by the functional value $Z = \int \mathcal{D}\psi e^{-\beta F[\psi(\mathbf{x})]}$ of the Ising system. An effective Hamiltonian over a continuum field $\psi(\mathbf{x})$ may now be written as[1]:

$$F[\psi(\mathbf{x})] = \int \mathrm{d}^d x \left[\frac{1}{2} w (\nabla\psi)^2 + f_L(\psi)\right];\ f_L = \frac{1}{2}a\psi^2 + \frac{1}{4}b\psi^4 - h\psi, \tag{11}$$

with $a = \sum_j K_{ij}\psi_j(1 - \sum_j K_{ij}\psi_j)/\beta v_0$ and $b = (\sum_j K_{ij}\psi_j)^4/3\beta v_0$ having non-zero minima $\psi_0 = \pm\sqrt{-a/b}$, along with $(\sum_j K_{ij}\psi_j)h/v_0 \to h$ and $w/\beta v_0 \to w = (1/2d)\sum_j \mathbf{R}_{0j}^2 K_{0j}$ for a d-dimensional macroscopic system. The resulting spontaneously broken symmetry is referred to as a "Mexican hat" potential and has a minimum region comprising a circle about the central peak of the local maximum[15].

3.3 Invariants

For electrons in a uniform magnetic field it is possible to write the 2D Schrödinger equation in terms of the nth level Landau energy as:

$$H(\mathbf{k})\left|u_{n\mathbf{k}}\right\rangle = E_n\left|u_{n\mathbf{k}}\right\rangle, \tag{12}$$

where $H(\mathbf{k}) = \frac{1}{2m}(-i\hbar\nabla + \hbar\mathbf{k} + e\mathbf{A})^2 + V(x,y)$, for some periodic potential $V(x,y)$. The *Integral Quantum Hall Conductivity* is then realised as a product of the Chern number n associated with the principal $U(1)$ bundle over the magnetic Brillouin zone, given as[15]:

$$\sigma_{xy} = n\frac{e^2}{h} \to \frac{e^2}{h}\sum_n \nu_n, \tag{13}$$

for some Hamiltonian $H(\mathbf{k}) = \boldsymbol{h}(\mathbf{k})\cdot\boldsymbol{\sigma}$, for which the contribution ν_n of the nth occupation band encircling the Brillouin zone is the Berry phase[4]:

$$\nu_n = -\frac{1}{2\pi}\oint_{\partial_{BZ}} \mathrm{d}\mathbf{k}\cdot\mathcal{A}^n(\mathbf{k}) = -\frac{\gamma_n[\partial_{BZ}]}{2\pi}. \tag{14}$$

It can be helpful to consider this nth band Chern number in terms of the region of the Brillouin zone for which the Berry connection can be smoothly defined with a transition function winding number around a given path $\mathcal{C}$:

$$\nu_n = \frac{1}{2\pi}\oint_{\mathcal{C}} \mathrm{d}\mathbf{k}\cdot\nabla_\chi(\mathbf{k}). \tag{15}$$

4 Phase Topology and Order

We distinguish quantum phases based upon their topological properties[15]. The basis upon which topological states are classified is a hierarchy composed of entanglement, symmetry, and topology. Of these, entanglement bears the least resemblance to classical physics and is sensitive to quantum statistics. Phases such as fractional quantum Hall states have ground states which are deeply entangled, making them impossible to classify solely by Landau symmetry rules.

4.1 Quantised Entanglement Entropy

We can classify the phases of the entangled gapped ground states of such systems by examining whether they are connected by *local unitary evolution*, which can be used to define an equivalence class if and only if they are in the same phase. However, it is possible to quantitatively measure entanglement in terms of its *topological entanglement entropy*, as proposed by Kitaev and Preskill[11]. The usual Von Neumann quantity of entropy associated with the partial traces of two subsystems A and B is recast as a linear element along the length of a large boundary L as:

$$S = \alpha L - \gamma + \mathcal{O}(L^{-1}). \tag{16}$$

For an asymptotic degeneracy per particle of a system consisting of N type-a quasiparticles, d_a, the total quantum dimension is given as $\gamma = \log \mathcal{D} = \log\sqrt{\sum_a d_a^2} = \log\sqrt{q}$. A fractional quantum Hall system with a filling factor defined by $\nu = 1/q$ has an odd number q distinct *Abelian anyons* and will always have quantum dimension equal to 1. *Non-Abelian anyons* may have a quantum dimension in excess of 1, although this number may not necessarily be an integer. Topological ordering is an important factor in the classification of *short-range entangled states* which are characterised according to distinct sets of topological invariants like compact manifold ground state degeneracies. FQH states are an example of such "standard" topologically ordered spaces.

States which have distinct topological properties but unbroken symmetries are called *symmetry-protected topological* phases[15]. Examples of such SPT phases include non-interacting topological insulators and semi-conductors. A gapped quantum phase is the equivalence class of ground states which are continuously deformed into one another by the variation of one or more of the parameters of a local Hamiltonian such that the non-zero energy gap for all excitations above the ground state is maintained. This sort of order is not equivalent to any classification related to the spontaneous symmetry breaking of a local order parameter[6].

The most essential characteristic of topological ordering is long-range entanglement. Typically the ground state degeneracy of systems defined on compact manifolds such as the torus is associated with the symmetry that can not be lifted by local perturbation. These topologically ordered state excitations are created by infinite products of local state operators which have intrinsically non-trivial and non-local statistical properties. As such, the spatially compact dynamics of the system depends upon low-energy deformations in the framework of the underlying topological field theory, including the non-local field excitations and ground state degeneracy; all of which stem from long-range topological order stemming from correlation of local operators from non-local sources.

It is also possible for topological phases to split into numerous *symmetry enriched topological phases* in presence of global symmetries in which the relationship between topology and symmetry gives rise to emergent excitations of non-local quasiparticles corresponding to the fractional charge numbers of the global symmetry group[9].

4.2 Toric Codes

For a 2D $(m \times n)$-lattice with $m \leq n$ it is possible to define an exactly solvable code which provides a canonical example of a topological phase[15] for a spin-1/2 model defined on a surface of genus g. *Toric codes* reveal the underlying topological order of a spin liquid in a highly entangled topological state.

These emergent states can be described as Abelian anyons and define the simplest example of a so-called *quantum double* which may serve a prototypical example of a *quantum error correction stabiliser code.* If we consider a set of spin-1/2 links of a 2D square lattice defined as the degrees of freedom of the spin operator $\boldsymbol{\sigma}_i = (\sigma_i^x, \sigma_i^y, \sigma_i^z)$ then we can physically interpret the vertex or star operator as A_v on the vertices of the lattice and the plaquette operator B_p as the products of the Pauli operator X and Z gates, respectively, then we may define the toric code as the Hamiltonian:

$$H_{\mathrm{tc}} = -J \sum_v \prod_{i \in v} \sigma_i^x - K \sum_p \prod_{i \in p} \sigma_i^z \tag{17}$$

$$= -J \sum_v A_v - K \sum_p B_p, \tag{18}$$

which is summed over all sites v and plaquettes p for the positive couplings J and K. All stars and plaquette operators commute with each other, and the minimal energy loss of the many-body states are identified as the eigenstates of A_v and B_p with $+1$ eigenvalues for each star and plaquette. For every state $|\mathbf{s}\rangle = |s_1 \cdots s_N\rangle$ having the property $\sigma_j^x |\mathbf{s}\rangle = s_j |\mathbf{s}\rangle$ having an even number of negative eigenvalues $s_j = -1$ for every star v satisfying the relation $\prod_{j\in v} s_j = 1$ with each link by necessity forming closed loops[8].

By choosing one star or plaquette to be negative it is possible to generate a toric code corresponding to the lowest energy excitations for quasiparticles describing electric, e, and magnetic, m interactions. Depending on the choice of gate it is possible to generate a pair of each type of each particle, with Z gate operations corresponding to electric particles and X gate operation corresponding to magnetic particles, respectively, such that we may define the ground state path operators[10]:

$$W_\gamma^{(e)} = \prod_{j\in\gamma} \sigma_j^z, \quad W_\gamma^{(m)} = \prod_{j\in\gamma} \sigma_j^x, \tag{19}$$

with a path between vertex sites v_i defined as γ, and where γ^* is a dual lattice path between p_i plaquettes.

5 Majorana Zero Modes

Non-Abelian anyons obey Pauli statistics involving non-commutative geometrical quantities such as the path ordering operator $\mathcal{P}$ over a projective Hilbert space, as seen in the earliest section. Majorana fermions are electromagnetically neutral particles having the highly unique characteristic of possessing a hermitian conjugate adjoint operator which is identical to its own complex representation, forming a unitary operator from the product of the two respective conjugate particles in their own right[2].

While no known elementary particle has ever been observed, there are numerous experimental confirmations of pseudo-physical Majorana modes present as emergent phenomena in condensed matter physics. These quasiparticle excitations of many-body systems occur in many TQC scenarios, specifically along the boundaries between qubits separated by time reversible space-time histories. If we denote γ_j to be an operater on the space of real numbers and $\gamma_j^\dagger$, its antiparticle, defined such that $\gamma = \gamma_j^\dagger$ for $\gamma^2 = 1$. We find the anti-commutation relation of these arbitrary perturbations of the massless and chargeless fermionic field operator to be given as $\{\gamma_i, \gamma_j\} = 2\delta_{ij}$ which emphasises the *propagating modes* that in the presence of an infinite potential[15] reduce to a gapless quantum operator corresponding to a number $\gamma_k = \sum_j e^{ijk}\gamma_j$ that must necessarily satisfy a "Majorana condition" in which the time-charge-inverse of the standard Fermionic operator corresponds to the Majorana zero conjugate for the kth state vector as $\gamma_{\mathbf{k}}^{\dagger} = \gamma_{\mathbf{k}}$, the canonical nature of which expresses the redundant description of the Bogoliubov-de Gennes formalism for the time-independent Hamiltonian for the n-integer labled quasiparticle energies for the 4-vector $\psi_n(\mathbf{r})$ written as:

$$\mathcal{H}_{\mathrm{BdG}}\psi_n = E_n\psi_n. \tag{20}$$

The physical realisation of these hole-anti-hole symmetries between superconducting microstates along wires have it that the band energies of a given energy mode correspond to the eigenvalue solutions of the eigenfunctions satisfying $E_{-n} = -E_n$.

6 Final Thoughts

Topological Quantum Computing represents, in so many ways, an intellectual and conceptual shift in the overall framework and formalism of Quantum Computing as a whole, while in a sense being a reduction of the notion of computing itself to a natural extension of the already well-established theory of electrodynamics. Whether or not Majorana fermions may (or may not!) reveal themselves as fundamental "states" of "matter" (in the absolute, most conventional sense), it is clear that the effective condensed matter field observables presenting themselves in practical quantum computing do conform to theoretical and measurable expectations of the Pauli statistics obeying the overall geometric quantities predicted by the approach.

While it may be somewhat far off in the future that topological quantum computers absolutely overtake the current paradigm of sub-milli-qubit superconducting quantum computational apparata, let alone the greater world of classical computing as a whole, we remain absolutely confident of the viability of the non-Abelian anyonic statistical universal quantum computer. As advancements are made in the production of mega-qubit systems leveraging poly-modal ion-photo trapped topological semi-conductors, the utility of this approach will become much more apparent and significant. Nature, herself, is a Topological Quantum Computer.

Addendum: Simulations of TQC

Following the procedure outlined in the important paper[14] concerning the simulation of correctly topologically ordered states on a noisy superconducting quantum processor, we have undertaken a numerical reproduction of several of the theoretical results discussed in the paper. Given below are excerpts from the QisKit simulations.

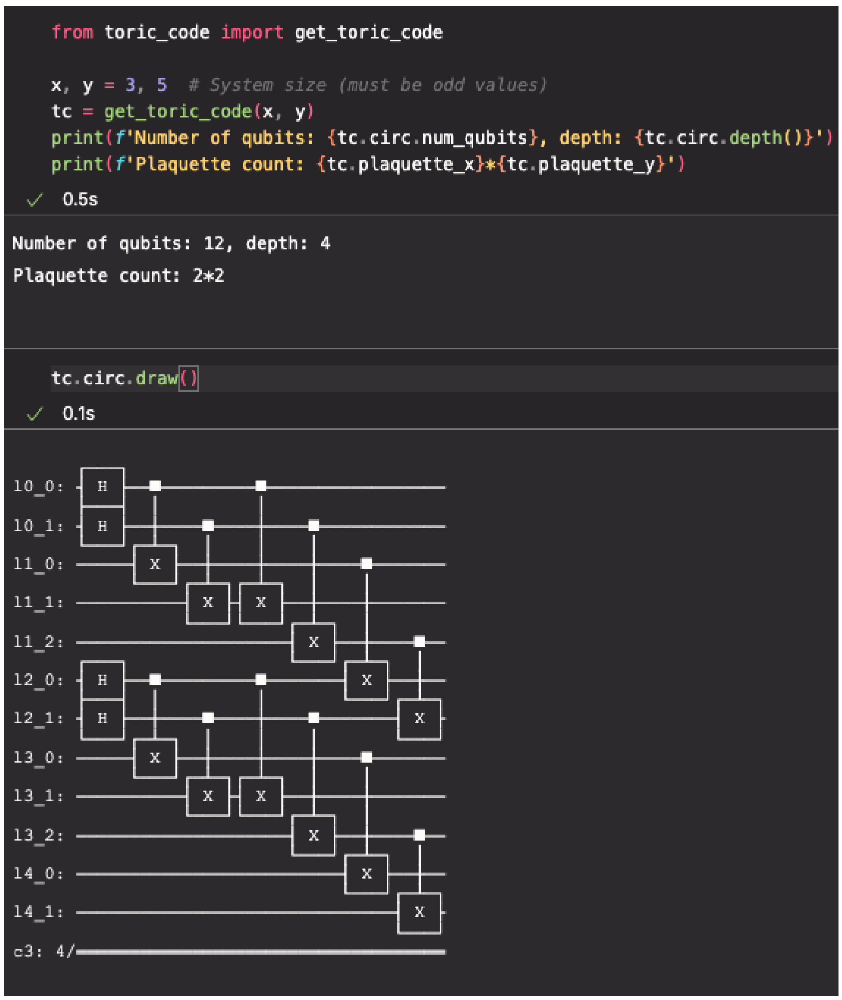

Figure 1: Ground state Toric code configuration given for (3,5)-system

```python
from toric_code_tests.test_init import get_plaquette_ev

import numpy as np
from qiskit import Aer
from qiskit import transpile

from toric_code import get_toric_code
from toric_code_matching import get_star_matching
```
✓ 0.4s

```python
# Use Aer's simulator
backend = Aer.get_backend('aer_simulator')
```
✓ 0.2s

```python
px, py = tc.plaquette_x, tc.plaquette_y

for i in range(px):
    for j in range(py):
        ev = get_plaquette_ev(backend, (x, y), (i, j))
        print(f'Plaquette ({i},{j}): {ev}')
```
✓ 0.2s

```
Plaquette (0,0): 1.0
Plaquette (1,0): 1.0
```

Figure 2: Plaquette calculation for a (3, 5)-system

```python
from toric_code_tests.test_init import get_star_ev

sx, sy = tc.star_x, tc.star_y

for i in range(sx):
    for j in range(sy):
        if len(get_star_matching(i, j, tc.y, tc.x)) < 4:
            continue

        ev = get_star_ev(backend, (x, y), (i, j))
        print(f'Star ({i},{j}): {ev}')
```
✓ 0.7s

```
Star (1,2): 1.0
```

Figure 3: Star calculation for a (3, 5)-system

```
100%|██████████| 729/729 [01:42<00:00,  7.08it/s]
100%|██████████| 729/729 [00:00<00:00, 37731.04it/s]
100%|██████████| 729/729 [00:00<00:00, 34388.05it/s]
100%|██████████| 729/729 [00:00<00:00, 22189.83it/s]
100%|██████████| 729/729 [00:00<00:00, 1715.12it/s]
100%|██████████| 729/729 [00:00<00:00, 1620.85it/s]
100%|██████████| 729/729 [00:00<00:00, 2130.50it/s]
100%|██████████| 729/729 [00:06<00:00, 113.68it/s]

Theoretical value of S/ln(2): 2.0. Measured value: 1.9989039443131724
Theoretical value of S/ln(2): 2.0. Measured value: 1.998862511831537
Theoretical value of S/ln(2): 2.0. Measured value: 1.9989134521780958
Theoretical value of S/ln(2): 4.0. Measured value: 3.9768822064841984
Theoretical value of S/ln(2): 3.0. Measured value: 2.988833875964967
Theoretical value of S/ln(2): 4.0. Measured value: 3.9779684602162515
Theoretical value of S/ln(2): 4.0. Measured value: 3.9063601354648387
Theoretical value of Stopo/ln(2): -1. Measured value: -1.0406444988777723
```

Figure 4: Measurement of Topological Entanglement Entropy for all Pauli basis combinations ($\mathcal{O}(3^6)$)

```python
for sq in [(0, 2), (0, 3), (2, 2), (2, 1)]:
    tc = get_toric_code(x, y, classical_bit_count=1, ancillas_count=1)

    x_string = [(2, 1), (2, 2)]
    create_e_particles(tc, x_string)

    z_string = [(1, 4), (0, 3), (1, 3)]  # , (0,2), (1,2)]
    create_m_particles(tc, z_string)

    tc.circ.h(tc.ancillas[0])
    apply_cxxxx_on_square(tc, sq)
    tc.circ.h(tc.ancillas[0])

    tc.circ.measure(tc.ancillas[0], 0)
    Nshots = 10000
    job = backend.run(transpile(tc.circ, backend), shots=Nshots)
    result = job.result()
    counts = result.get_counts(tc.circ)

    if '0' not in counts:
        counts['0'] = 0
    if '1' not in counts:
        counts['1'] = 0

    cos_theta = (counts['0'] - counts['1']) / Nshots
    expected_res = -1. if sq in [(0, 2), (0, 3)] else 1.
    print(f'Expected value of cos(theta): {expected_res}. Measured value: {cos_theta}')
```

```
Expected value of cos(theta): -1.0. Measured value: -1.0
Expected value of cos(theta): -1.0. Measured value: -1.0
Expected value of cos(theta): 1.0. Measured value: 1.0
Expected value of cos(theta): 1.0. Measured value: 1.0
```

Figure 5: Extraction of Braiding Statistics from simulated 2-Qubit Majorana fermions with matching toric codes

References

[1] Stefan Backens, Alexander Shnirman, Yuriy Makhlin, Yuval Gefen, Johan E. Mooij, and Gerd Schön, *Emulating majorana fermions and their braiding by ising spin chains*, Phys. Rev. B **96** (2017), 195402.

[2] Prabhakar Bandaru and Shreyam Natani, *Topological states for new modes of information storage and transfer: A survey of the status of the discovery of the majorana modes in the solid state*, pp. 99–100, Springer International Publishing, 2022.

[3] Timothy Boyer, *Classical electromagnetism and the aharonov–bohm phase shift*, Foundations of Physics **30** (2000), 907–932.

[4] Huai-Chun Chang and Hsiu-Chuan Hsu, *Digital quantum simulation of dynamical topological invariants on near-term quantum computers*, 2021.

[5] Kartik Chhajed, *From the ising model to kitaev chain - an introduction to topological phase transitions*, (2020).

[6] Tianxiang Dai, Yutian Ao, Jueming Bao, Jun Mao, Yulin Chi, Zhaorong Fu, Yilong You, Xiaojiong Chen, Chonghao Zhai, Bo Tang, Yan Yang, Zhihua Li, Luqi Yuan, Fei Gao, Xiao Lin, Mark G. Thompson, Jeremy L. O'Brien, Yan Li, Xiaoyong Hu, Qihuang Gong, and Jianwei Wang, *Topologically protected entanglement emitters*, Conference on Lasers and Electro-Optics, Optica Publishing Group, 2022, p. FW1A.1.

[7] Alvaro Ferraz, Kumar S. Gupta, Gordon Walter Semenoff, and Pasquale Sodano (eds.), *Strongly coupled field theories for condensed matter and quantum information theory*, Springer International Publishing, 2020.

[8] Keisuke Fujii, *Quantum computation with topological codes: from qubit to topological fault-tolerance*, 2015.

[9] Yichen Huang, *Entanglement dynamics from random product states: Deviation from maximal entanglement*, IEEE Transactions on Information Theory **68** (2022), no. 5, 3200–3207.

[10] Kyusung Hwang, Ara Go, Ji Heon Seong, Takasada Shibauchi, and Eun-Gook Moon, *Identification of a kitaev quantum spin liquid by magnetic field angle dependence*, Nature Communications **13** (2022), no. 1.

[11] Alexei Kitaev and John Preskill, *Topological entanglement entropy*, Phys. Rev. Lett. **96** (2006), 110404.

[12] Ville Lahtinen and Jiannis Pachos, *A short introduction to topological quantum computation*, Sep 2017.

[13] J.J. Rotman, *An introduction to homological algebra*, Universitext, Springer New York, 2008.

[14] K. J. Satzinger, Y.-J Liu, A. Smith, C. Knapp, M. Newman, C. Jones, Z. Chen, C. Quintana, X. Mi, A. Dunsworth, C. Gidney, I. Aleiner, F. Arute, K. Arya, J. Atalaya, R. Babbush, J. C. Bardin, R. Barends, J. Basso, A. Bengtsson, A. Bilmes, M. Broughton, B. B. Buckley, D. A. Buell, B. Burkett, N. Bushnell, B. Chiaro, R. Collins, W. Courtney, S. Demura, A. R. Derk, D. Eppens, C. Erickson, L. Faoro, E. Farhi, A. G. Fowler, B. Foxen, M. Giustina, A. Greene, J. A. Gross, M. P. Harrigan, S. D. Harrington, J. Hilton, S. Hong, T. Huang, W. J. Huggins, L. B. Ioffe, S. V. Isakov, E. Jeffrey, Z. Jiang, D. Kafri, K. Kechedzhi, T. Khattar, S. Kim, P. V. Klimov, A. N. Korotkov, F. Kostritsa, D. Landhuis, P. Laptev, A. Locharla, E. Lucero, O. Martin, J. R. McClean, M. McEwen, K. C. Miao, M. Mohseni, S. Montazeri, W. Mruczkiewicz, J. Mutus, O. Naaman, M. Neeley, C. Neill, M. Y. Niu, T. E. O'Brien, A. Opremcak, B. Pató, A. Petukhov, N. C. Rubin, D. Sank, V. Shvarts, D. Strain, M. Szalay, B. Villalonga, T. C. White, Z. Yao, P. Yeh, J. Yoo, A. Zalcman, H. Neven, S. Boixo, A. Megrant, Y. Chen, J. Kelly, V. Smelyanskiy, A. Kitaev, M. Knap, F. Pollmann, and P. Roushan, *Realizing topologically ordered states on a quantum processor*, Science **374** (2021), no. 6572, 1237–1241.

[15] Tudor D. Stanescu, *Introduction to topological quantum matter quantum computation*, CRC Press, 2020.

[16] Yijia Wu, Haiwen Liu, Jie Liu, Hua Jiang, and X C Xie, *Double-frequency Aharonov-Bohm effect and non-Abelian braiding properties of Jackiw-Rebbi zero-mode*, National Science Review **7** (2019), no. 3, 572–578.

[17] Zedong Yang, Brett Heischmidt, Sasa Gazibegovic, Ghada Badawy, Diana Car, Paul A. Crowell, Erik P.A.M. Bakkers, and Vlad S. Pribiag,

Spin transport in ferromagnet-InSb nanowire quantum devices, Nano Letters **20** (2020), no. 5, 3232–3239.